remote sensing

Article

A Migratory Biomass Statistical Method Based on High-Resolution Fully Polarimetric Entomological Radar

Teng Yu [1,2], Muyang Li [1], Weidong Li [1,2,*], Tianran Zhang [1], Rui Wang [1,2] and Cheng Hu [1,2]

[1] School of Information and Electronics, Beijing Institute of Technology, Beijing 100081, China
[2] Advanced Technology Research Institute, Beijing Institute of Technology, Jinan 250300, China
* Correspondence: lwd.bit@bit.edu.cn

Abstract: Entomological radar is a specially designed instrument that can measure the behavioral and biological characteristics of high-altitude migrating insects. Its application is of great significance for the monitoring, early warning, and control of agricultural pests. As an important component of the local migratory biomass, insects fly in the air during the day and night. The fully polarimetric entomological radar was carefully designed with all-day, all-weather, and multi-function measurement capabilities. The fully polarimetric entomological radar measures the mass of a single insect based on the radar cross-sectional (RCS) measurement and then calculates the biomass of migrating insects. Therefore, the measurement accuracy of the insect RCS is the key indicator affecting the accuracy of migratory biomass statistics. Due to the radar's lack of in-beam angle measurement ability, the insect RCS is usually measured based on the assumption that the insect is on the beam center. Therefore, the measured RCS will be smaller than true value if the insect deviates from the beam center due to the gain curve of the antenna. This leads to measurement errors in regard to the insect mass and migratory biomass. In order to solve this problem, a biomass estimation method, reported in this paper, was designed under the assumption of a uniform distribution of migrating insects in the radar monitoring airspace. This method can estimate the individual RCS expectation of migrating insects through a statistical method without measuring the position of the insects in the beam and then obtain the migratory biomass. The effectiveness of the model and algorithm is verified by simulations and entomological radar field measurements.

Keywords: entomological radar; insect RCS measurement; migratory biomass measurement; insect mass measurement

check for updates

Citation: Yu, T.; Li, M.; Li, W.; Zhang, T.; Wang, R.; Hu, C. A Migratory Biomass Statistical Method Based on High-Resolution Fully Polarimetric Entomological Radar. *Remote Sens.* **2022**, *14*, 5426. https://doi.org/10.3390/rs14215426

Academic Editor: Dusan Gleich

Received: 9 October 2022
Accepted: 25 October 2022
Published: 28 October 2022

Publisher's Note: MDPI stays neutral with regard to jurisdictional claims in published maps and institutional affiliations.

Copyright: © 2022 by the authors. Licensee MDPI, Basel, Switzerland. This article is an open access article distributed under the terms and conditions of the Creative Commons Attribution (CC BY) license (https://creativecommons.org/licenses/by/4.0/).

1. Introduction

According to research, latitudinal migrations of vast numbers of flying insects, birds, and bats [1–8] lead to huge seasonal exchanges of biomass and nutrients across the Earth's surface [8–11]. Because many migrant species (particularly insects) are extremely abundant, seasonal migrations can profoundly affect communities through predation and competition while transferring enormous quantities of energy, nutrients, propagules, pathogens, and parasites between regions, with substantial effects on essential ecosystem services, processes, biogeochemistry [8–11], and, ultimately, the ecosystem function. In addition, China uses 7% of the world's arable land to feed 22% of the world's population [12]. However, many potential threats limit grain production, including diseases, pests, and weeds. According to statistics, various diseases, insect pests, and weeds have reduced the global crop production by more than 40% [12]. Most of this production reduction is caused by seasonal pests [13–15]. Consequently, biomass explorations in the field of scientific research are of great interest for the fields of migratory biology, feeding biology, fly biology, reproductive biology, and green control techniques.

Entomological radar is one of the most effective tools, with a multi-function capacity and the ability to work in all weather and day conditions. Entomological radar first

appeared in the 1960s. It was successfully developed by the British locust control center (ALRC) for the first time [16,17]. After more than half a century of development, the new fully polarimetric entomological radar can accurately evaluate the migration biomass to provide effective data supporting the accurate control of migration pests and macro-migration biology research [18–21]. Fully polarimetric entomological radar can simultaneously radiate signals with perpendicular polarizations and orthogonal waveforms. The radar receives the target echo and demodulates the orthogonal signal to obtain the full polarization information on the insects. Compared with traditional VLR-type entomological radar using a rotated single-polarization feed, it has the advantage of being able to measure the target instantaneous polarization information. Insect migratory biomass refers to the total mass of insects crossing a certain area in a certain period. When measuring the migratory biomass, the RCS of the insect, in which its body axis is perpendicular to the polarization direction, is first calculated and recorded as v. Then, the insect mass is estimated based on the empirical equation that is fitted with a large number of insect specimens measured in laboratory [22,23]. The estimation requires the entomological radar to have a high RCS measurement accuracy [24]. When an insect traverses the radar beam, the traversing position is random, and the insect only has a very small probability of traversing the center of the radar beam. Therefore, most of the RCS measurements are relatively small, which leads to the distortion of the insect mass estimation [25–27]. A traditional VLR-type radar can effectively solve this problem by the rotating polarization and nutation method [21]. However, in fully polarimetric entomological radar, this problem has not been solved effectively. This scenario cannot meet the requirements for the high-precision measurement of the insect mass, thus increasing the statistical error of the migrating biomass.

In order to solve this problem in the fully polarimetric entomological radar system, this paper presents a method based on the assumption that insects are evenly distributed in the same height layer when flying within the radar detectable area. Instead of obtaining the angle information of each insect in the beam, the biomass for this migration can be obtained by statistical estimation. In this method, the spatial model of the insect traversing beam is first established, and the reasonable assumption is formed based on the location of the traversing beam of the migrating insect species. The estimation method of the RCS expectation is deduced, which reduces the measurement error obtained using radar without the capacity for in-beam angle measurement. Then, the insect mass estimation method is used to estimate the insect mass expectation. Finally, the airspace-wide biomass is estimated with the information about the migratory flux. A simulation was conducted to analyze the effect of the insect number on the accuracy of the proposed method. The field test was conducted with a Ku-band, high-resolution, fully polarimetric entomological radar without the capacity for in-beam angle measurement to validate the proposed method.

The structure of the subsequent sections is as follows: Section 2 presents the spatial model of the insect traversing beam based on the characteristics of the migration of the insect population. A new method for estimating RCS expectations is proposed so as to estimate the mass expectations of migrating insects. Finally, the biomass of the migrating insects is estimated in combination with the results for the migratory flux. In Section 3, the traditional method and the new method are used to calculate the expected value of the RCS and the biomass of the migratory insects, respectively, which verified the advantages of the new method. The field experimental data measured with the Ku-band fully polarimetric entomological radar are used to validate the effectiveness of the proposed method in Section 3. Sections 4 and 5 discuss the results and provide the conclusion of the paper.

2. Method of Calculating Migratory Biomass

2.1. Model of Biomass Measurement

In this section, a model is established to calculate the biomass through the flux. In a migration event, if this target event is an intense migration event, where the given species largely dominates among migrating insects, the biomass of these insects can be estimated directly. If there are several species of insects involved in this migration, a preliminary

classification of all the measurements of the insect targets is required. In their study [19], Cheng Hu et al. introduced the method of insect classification based on information such as the wingbeat frequency and body-length-to-width ratio measured by a fully polarimetric entomological radar. This paper assumes that the insects are of the same species and that the RCS follows a normal distribution.

As shown in Figure 1, the entomological radar usually works in the vertical-looking mode. In this mode, the radar beam is adjusted vertically to the sky. The blind range of the entomological radar is $R_{\min}$, and the farthest detection range is $R_{\max}$. Suppose that Num insects migrate across the radar beam and are measured by the radar within a period of time T. The measured insect mass sequence is $(m_1, m_2 \ldots m_{Num})$, and the calculation formula of the insect migratory biomass M is as follows:

$$M = \sum_{i=1}^{Num} m_i \tag{1}$$

Equation (1) can also be equated with the product of the number of migrating insects and the average mass, i.e.,

$$M = Num \times E(m_i) \tag{2}$$

where $E(m_i)$ denotes the average value of the individual insect mass. In radar applications, due to the limited radar beam coverage, if we want to estimate the migratory biomass in a larger area, the migratory biomass can be estimated according to the migratory flux and crossing area. As shown in Figure 2, within a regional range L, the schematic represents a horizontal scale of a uniform migration event on a monitoring plane, including the radar beam. The radar works in the vertical-looking mode, and the detection range of the radar is H. Due to the narrow radar beam, if only the insects measured by the radar are counted as the estimation results of the migratory biomass, it is obviously unable to represent the real biomass scale. The $H \times L$ plane is defined as perpendicular to the migration direction. Then, suppose that the migrating species of insects occur uniformly in the L axis of the plane. This means that we can take any distance ΔL in L, and the migratory flux is consistent. The migratory flux of the insects, $Flux$, is expressed as the number of insects per unit time and unit area. It represents the flow of the migrating insects [20,21], and its calculation method is described in detail in [28].

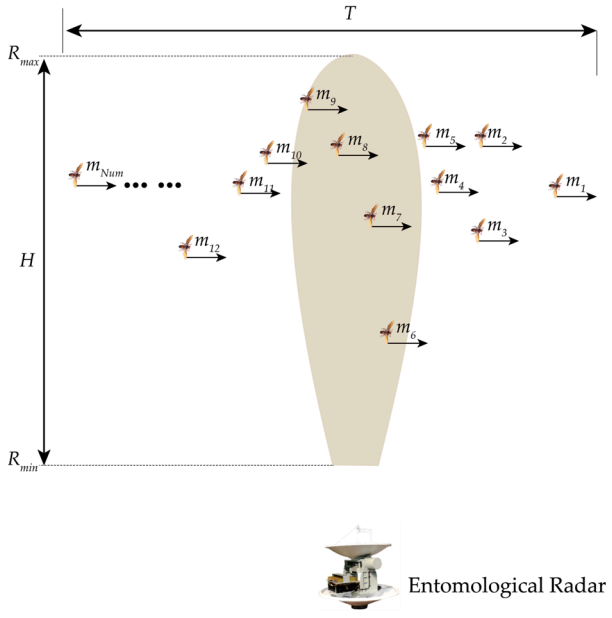


Figure 1. Schematic diagram of the migratory biomass.

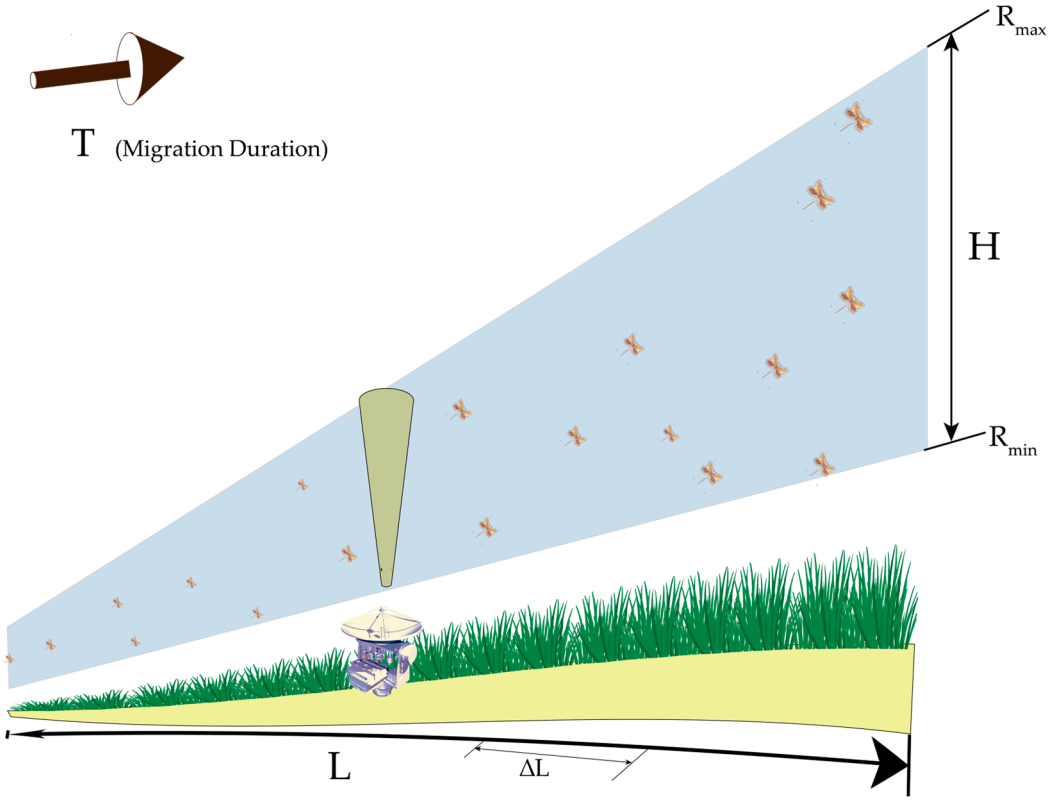


Figure 2. Schematic diagram of the biomass measurement on a larger geographical scale.

Within the airspace area $L \times H$, the approximate calculation formula of the migratory biomass is as follows:

$$M = Flux \times T \times H \times L \times E(m_i) \tag{3}$$

where T denotes the statistical period of the insect migration. H denotes the altitude range measured by the radar. L indicates the statistical regional range. *Flux* represents the insect migratory flux within the radar detection coverage. When the radar works in the vertical-looking mode, the insect migratory *flux* calculation method is described as follows. Firstly, the radar detection airspace is divided into the (1,2...n...N) N-th equal-height and (1,2...k...K) K-th equal-length time intervals. The altitude interval is Δh, and the time interval is ΔT. In the minimum statistical unit (k, n), $num_{k,n}$ migrating insects were detected, and then the flux statistics $flux(k, n)$ can be calculated as:

$$flux(k, n) = \frac{1}{\Delta h \Delta T} \sum_{i=1}^{num_{k,n}} \frac{1}{D_i(k, n)} \tag{4}$$

In Equation (4), $D_i(k, n)$ indicates the tangential distance over which each insect can be detected if it crosses the center of the beam [28]. Further, in the radar detectable airspace, the migrating flight flux parameter *Flux* over a period is calculated as follows:

$$\begin{aligned} Flux &= \frac{1}{NK} \sum_{k=1}^{K} \sum_{n=1}^{N} flux(k, n) \\ &= \frac{1}{NK} \sum_{k=1}^{K} \sum_{n=1}^{N} \left[\frac{1}{\Delta h \Delta T} \sum_{i=1}^{num_{k,n}} \frac{1}{D_i(k,n)} \right] \end{aligned} \tag{5}$$

2.2. Method of Biomass Calculation

In this section, the calculation method of the biomass is introduced in detail. In Equation (3), the mass expectation of an individual insect $E(m_i)$ should be calculated.

Entomological radar can measure the mass of a single insect by measuring the RCS of the insect. In this research field, Anthony C. Aldhous introduced the relationship between the insect RCS and its mass in his Ph.D. thesis [29] and formed a fitting curve, which proved the feasibility of inverting the insect mass from the RCS results detected by entomological radar. In recent years, Hu Cheng et al. introduced a method of measuring the insect polarization scattering matrix (PSM) with fully polarimetric entomological radar to obtain polarization invariants, used to for invert the insect mass in [30,31]. The principle works on the basis that after the insect PSM is obtained, the insect polarization invariant factor v is calculated, and the corresponding relationship between v and the insect mass is obtained by the sample measurement and curve fitting [32]. The physical meaning of the polarization invariant v is the RCS, with the insect body axis perpendicular to the polarization direction. In this paper, the calculation method of v is given directly, and the derivation process is not described in detail. Suppose the insect PSM is represented by a matrix variable $\mathbf{S}$, so that $\mathbf{S}$ is [33]:

$$\mathbf{S} = \begin{bmatrix} S_{HH} & S_{HV} \\ S_{VH} & S_{VV} \end{bmatrix} = \begin{bmatrix} A_{HH}e^{j\phi_{HH}} & A_{HV}e^{j\phi_{HV}} \\ A_{VH}e^{j\phi_{VH}} & A_{VV}e^{j\phi_{VV}} \end{bmatrix} \tag{6}$$

In Equation (6), in the subscripts of S_{xy}, A_{xy}, and $\varnothing_{xy}$, x indicates the polarization mode of the receiving channel, and y indicates the polarization mode of the transmitting channel. S_{xy} represents the complex value of the target echo intensities. A_{xy} and $\varnothing_{xy}$ represent the amplitude and phase of S_{xy}, respectively. S_{HV} and S_{VH} are identical in the monostatic radar system with respect to the reciprocity targets. The Graves power matrix is defined as [34]:

$$\mathbf{G} = \begin{bmatrix} g_{11} & g_{12} \\ g_{21} & g_{22} \end{bmatrix} = \mathbf{S}^H\mathbf{S} \tag{7}$$

In Equation (7), the "H" operation represents the conjugate transpose calculation. The polarization invariant v is calculated as:

$$v = \begin{cases} \frac{(g_{11}+g_{22}) + \sqrt{(g_{11}-g_{22})^2 + 4g_{12}g_{21}}}{2}; (\Delta\phi > 0) \\ \frac{(g_{11}+g_{22}) - \sqrt{(g_{11}-g_{22})^2 + 4g_{12}g_{21}}}{2}; (\Delta\phi < 0) \end{cases} \tag{8}$$

$\Delta\phi$ could be calculated as [18,30,31]:

$$\Delta\phi = \arg\left(\frac{\mu_1}{\mu_2}\right) \tag{9}$$

where $\arg(x)$ means that, when calculating the phase of x, μ_1 and μ_2 are the two eigenvalues of the PSM ($|\mu_1| \geq |\mu_2|$) [18,30,31]:

$$\begin{cases} \mu_1 = \frac{1}{2}\left(A_{HH}e^{j\phi_{HH}} + A_{VV}e^{j\phi_{VV}}\right) + \frac{1}{2}\sqrt{\left(A_{HH}e^{j\phi_{HH}} - A_{VV}e^{j\phi_{VV}}\right)^2 + 4A_{HV}A_{VV}e^{j(\phi_{HV}+\phi_{VH})}} \\ \mu_2 = \frac{1}{2}\left(A_{HH}e^{j\phi_{HH}} + A_{VV}e^{j\phi_{VV}}\right) - \frac{1}{2}\sqrt{\left(A_{HH}e^{j\phi_{HH}} - A_{VV}e^{j\phi_{VV}}\right)^2 + 4A_{HV}A_{VV}e^{j(\phi_{HV}+\phi_{VH})}} \end{cases} \tag{10}$$

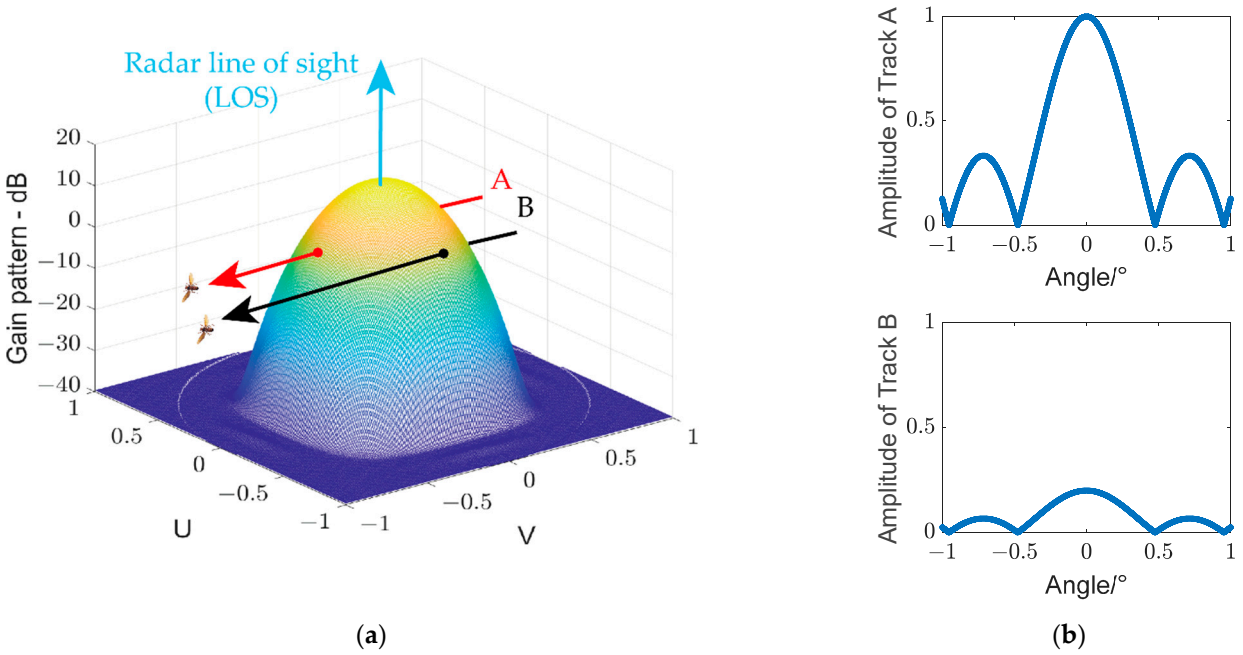
The empirical formula of the insect mass estimation based on v is written as [18,30,31]:

$$m = 10^{0.07(\lg v)^2 + 1.13\lg v + 5.51} \tag{11}$$

where $\lg v \in [-5.7, -3.4]$. Substituting Equation (11) into Equation (1), the biomass of the migrating insects measured by entomological radar is obtained. Therefore, the estimation of the migratory biomass can be completed by calculating the RCS of each insect perpendicular to the body axis, that is, the polarization invariant eigenvalue v.

For radar without the capacity for in-beam angle measurement, the RCS measurement value is often smaller than the true value, because the insect flight trajectory may not cross the radar beam center. It is assumed that two insects with the same scattering characteristics cross the radar beam at the same height but in different beam positions. Two tracks are

formed, as shown in Figure 3. Track A passes through the radar beam center, but track B does not, as shown in Figure 3a. The radar obtains two different target echo amplitude curves, in which the peak amplitude of track A is higher than that of track B, as shown in Figure 3b. Thereby, the RCSs measured by entomological radar are usually smaller than the true values, as are the estimated masses.



(**a**) (**b**)

Figure 3. Schematic diagram of the amplitudes of the echo signal of insects crossing the beam at different positions. (**a**) Schematic diagram of the different positions of insects crossing the radar beam. (**b**) Amplitude of the trajectories produced by different insects.

Although the accurate RCSs of individual insects are difficult to measure, the statistical mean value of v can be calculated based on the uniform distribution assumption. It should be noted that $E(m_i)$ is the mean weight of the insects of unique dominant species. By using the mean value, the mass expectation $E(m_i)$ can be calculated as:

$$E(m_i) = 10^{0.07(lg\bar{\delta})^2+1.13lg\bar{\delta}+5.51} \tag{12}$$

where $\bar{\delta}$ represents the mean value of v. Assuming that Num insects were measured in a statistical period, the RCS sequence can then be written as $(v_1, v_2 \ldots v_{Num})$, where v_i indicates the RCS v of the i-th insect. The mean value of the RCS $\bar{\delta}$, in this statistical period, should be calculated as:

$$\bar{\delta} = \frac{1}{Num}\sum_{i=1}^{N} v_i \tag{13}$$

In order to estimate $\bar{\delta}$, the position model of the insect crossing the beam is established. The model of an insect with a serial number i crossing the beam is developed, as shown in Figure 4. The radar position is defined as the point O, and the beam center at the insect's detected altitude R_i is O'. After the insect crosses the beam, the radar will obtain a series of P discrete amplitude points. The corresponding spatial position point is $\left(A_{i-1}, A_{i-2} \ldots A_{i-p} \ldots A_{i-P}\right)$, where subscript $p \in [1, P]$. When the insect is at the position point $A_{i-\max}$, the radar measures the strongest echo energy, which means the insect is closest to the center of the beam O', and the angle $\angle A_{i-\max}OO'$ is defined as $\gamma_{i-\max}$. When the i-th insect is at the A_{i-max} position, the echo of the insect is the strongest. Take the RCS measurement value of the insect, here, as v_i.

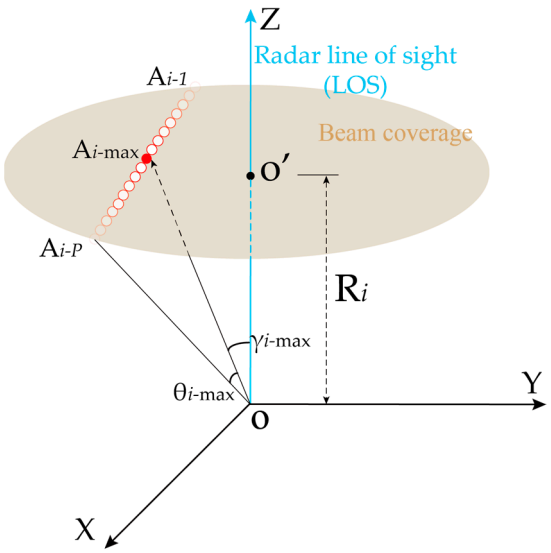


Figure 4. Insect crossing beam model diagram.

The entomological radar is able to directly acquire the signal-to-noise ratio (SNR) SNR_i of the insect at position $A_{i-\max}$. The RCS of the i-th insect v_i measurement decreases as γ becomes larger. Since v_i is obtained by calculating the radar equation, the simplified expression of the equation is:

$$v_i = \frac{R^4 \cdot SNR}{G^2 C} \tag{14}$$

In Equation (14), R is the range from the target to radar. SNR is the measured SNR. G is the antenna gain. According to the radar equation, the calculation equation of C is:

$$C = \frac{N_1 N_2 T_s D_c P_t \lambda^2}{(4\pi)^3 K T_0 F_n L'} \tag{15}$$

where N_1 and N_2 denote the number of frequency steps and the number of pulsed Doppler accumulation frames, respectively. T_s is the periodic sampling time. D_c is duty cycle of the radar transmit pulse. P_t is the maximum power of the radar transmitter. λ is the wavelength. K is the Boltzmann constant. T_0 is the ambient temperature during the radar operation. F_n is the radar receiver noise figure. L' is the loss of the radar transceiver link. The coefficient C is uniquely determined by the entomological radar hardware.

In Equation (14), there is a corresponding functional relationship between he antenna gain G and angle γ, i.e., $G = G_{\max} f_G(\gamma)$. When $\gamma = 0$, G reaches the peak. $f_G(\gamma)$ is the attenuation function of the antenna radiation energy. There are many types of antenna pattern approximation functions. In order to facilitate the calculation, the quadratic cosine function is selected as the approximate function of the antenna pattern attenuation in this paper. $f_G(\gamma)$ is defined as:

$$f_G(\gamma) = \begin{cases} \cos^2(k\gamma) & , |k\gamma| \leq \frac{\pi}{2} \\ 0 & , \text{else} \end{cases} \tag{16}$$

where $k = \pi(2\theta_{3dB})^{-1}$, and θ_{3dB} represents the radar half-power beam width. Insects are small targets. In most cases, they can only be detected when they cross the main lobe of the radar antenna, or when the angle included within the radar line of sight is small.

Therefore, it can be assumed that $|k\gamma_{i-\max}| \leq \pi/2$. According to Equation (14), the equation for calculating the insect RCS numbered i can be obtained as follows:

$$v_i = \frac{{R_i}^4 \cdot SNR_i}{\cos^4(k\gamma_{i-\max}) G_{\max}^2 C} \tag{17}$$

Substituting (17) into the definition Equation (13) of the average RCS:

$$\overline{\delta} = \frac{1}{N} \sum_{i=1}^{N} \frac{{R_i}^4 \cdot SNR_i}{\cos^4(k\gamma_{i-\max}) G_{\max}^2 C} \tag{18}$$

In the traditional calculation method of fully polarimetric entomological radar, the attenuation function of the antenna radiation energy is ignored. This means that $\gamma_{i-\max}$ in Equation (18) is assumed to be 0, which will lead to large error in the statistical results of $\overline{\delta}$. In order to obtain more reasonable results, the following approximation is conducted:

$$\begin{aligned} \overline{\delta} &= \frac{1}{N} \sum_{i=1}^{N} \frac{{R_i}^4 \cdot SNR_i}{\cos^4(k\gamma_{i-\max}) G_{\max}^2 C} \\ &\approx \frac{1}{N} \sum_{i=1}^{N} \frac{{R_i}^4 \cdot SNR_i}{\mathrm{E}[\cos^4(k\gamma_{i-\max})] G_{\max}^2 C} \end{aligned} \tag{19}$$

The calculation of $\mathrm{E}[\cos^4(k\gamma_{i-\max})]$ is as follows. As shown in Figure 5, the length of the insect trajectory across the beam is defined as X_i, which is the distance from the first measurement point A_{i-1} to the last measurement point A_{i-P}. The closest distance to the beam center is defined as Y_i, which is the distance from O' to the point $A_{i-\max}$. The modulus of vector $\overrightarrow{O'A_{i-P}}$ is defined as $D_i/2$. The included angle $\angle A_{i-\max} O A_{i-P}$ is defined as $\theta_{i-\max}$. As can be seen from Figure 5, due to $R_i \gg Y_i$ and $\gamma_{i-\max}$, Y_i and R_i approximately have the following relationship:

$$\gamma_{i-\max} \approx \frac{Y_i}{R_i} \tag{20}$$

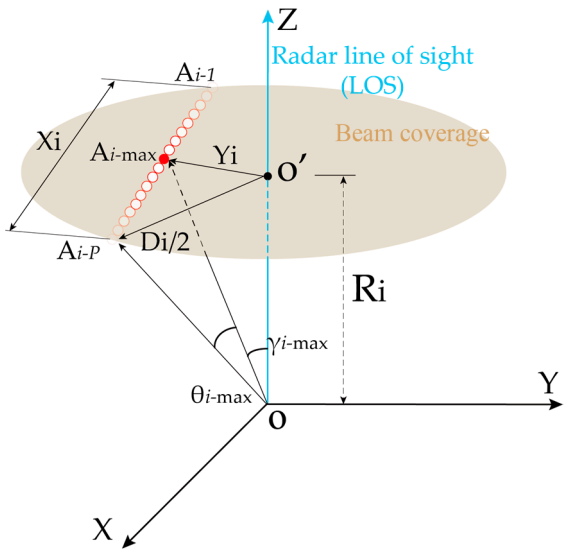


Figure 5. Schematic diagram of the insect location model.

It is assumed that at a certain height, the position of the insect crossing the beam is random. Therefore, the random variable Y_i obeys the uniform distribution of $\mathrm{U}[0, D_i/2]$.

That is, $\gamma_{i-\max}$ is a uniform distribution subject to $U[0, D_i/(2R_i)]$. Then, according to the equation of probability distribution function:

$$E\left[\cos^4(k\gamma_{i-\max})\right] = \int_0^{\frac{D_i}{2R_i}} \cos^4(k\gamma_{i-\max}) \frac{2R_i}{D_i} d\gamma_{i-\max} \tag{21}$$

Equation (21) can be simplified as:

$$E\left[\cos^4(k\gamma_{i-\max})\right] = \frac{3}{8} + \frac{R_i}{2D_i k} \sin\left(k\frac{D_i}{R_i}\right) + \frac{R_i}{16D_i k} \sin\left(k\frac{2D_i}{R_i}\right) \tag{22}$$

In Equation (22), R_i can be directly measured by entomological radar, and k is a fixed constant related to the radar beam width. The unknown variable D_i cannot be measured directly. This paper presents an estimation method which can estimate the expected value of D_i. The relationship between D_i and X_i is defined as $D_i = X_i/\mu_i$, and μ_i is named as the deviation coefficient. For each insect, X_i is a constant; therefore, it can be determined that:

$$E(\mu_i) = E\left(\frac{X_i}{D_i}\right) \tag{23}$$

As shown in Figure 5, from the trigonometric function relationship, it can be determined that:

$$X_i = \sqrt{{D_i}^2 - 4{Y_i}^2} \tag{24}$$

Divide both sides of Equation (24) by D_i:

$$\mu_i = \sqrt{1 - 4\left(\frac{Y_i}{D_i}\right)^2} \tag{25}$$

The right side of Equation (25) is the function of Y_i/D_i, and $E(Y_i/D_i) \in N[0, 0.5]$. Thus, it can be solved according to the definition of the probability distribution function:

$$\begin{array}{c} E(\mu_i) = \int_0^{\frac{1}{2}} 2\sqrt{1 - 4\left(\frac{Y_i}{D_i}\right)^2} d\left(\frac{Y_i}{D_i}\right) \\ = \frac{1}{2}\arcsin(1) = \frac{\pi}{4} \end{array} \tag{26}$$

Then, it can be determined that:

$$E(D_i) = \frac{4}{\pi} E(X_i) \tag{27}$$

In Equation (22), the expected value $E(D_i)$ of D_i is approximately used to replace D_i. Then, it can be determined that:

$$E\left[\cos^4(k\gamma_{i-\max})\right] = \frac{3}{8} + \frac{\pi R_i}{8kE(X_i)} \sin\frac{4kE(X_i)}{\pi R_i} + \frac{\pi R_i}{64kE(X_i)} \sin\frac{8kE(X_i)}{\pi R_i} \tag{28}$$

In the above equation, X_i of each insect can be calculated separately. According to the definition shown in Figure 5, the calculation method of X_i is:

$$X_i \approx 2\theta_{i-\max} R_i \tag{29}$$

When the insect crosses the radar beam, due to the directionality of the radar antenna, the SNR of the insect will undergo a process progressing from small to large and then small again. As shown in Figure 6, when the insect is at $A_{i-\max}$, the SNR is SNR_i, and $\theta = 0$. When the target is at A_{i-P}, the SNR is SNR_{min}, and $\theta = \theta_{i-\max}$.

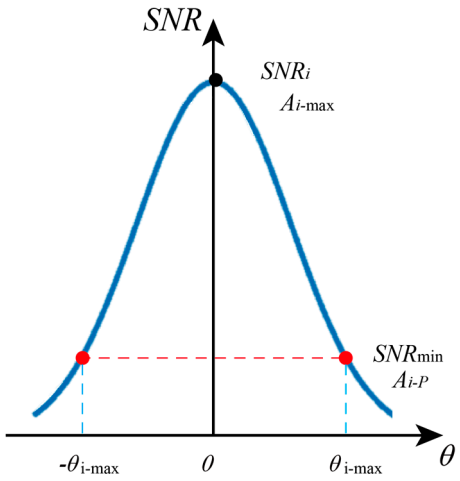


Figure 6. Relation curve between the target SNR and θ when the insect crosses the beam.

In Figure 6, $SNR_{\min}$ is the detection threshold, which is usually set as a constant. Therefore, in combination with Equation (11), it can be determined that:

$$\frac{SNR_i}{SNR_{\min}} = \frac{1}{{f_G}^2(\theta_{i-\max})} = \frac{1}{\cos^4(k\theta_{i-\max})} \tag{30}$$

where $\theta_{i-\max}$ can be calculated as:

$$\theta_{i-\max} = \frac{1}{k}\arccos\left(\frac{SNR_{\min}}{SNR_i}\right)^{\frac{1}{4}} \tag{31}$$

X_i can be calculated by substituting the above equation into Equation (29):

$$X_i \approx \frac{4R_i\theta_{3dB}}{\pi}\arccos\left(\frac{SNR_{\min}}{SNR_i}\right)^{\frac{1}{4}} \tag{32}$$

The value $\overline{\delta}$ can be obtained by connecting Equations (19), (32) and (28).

$$\overline{\delta} \approx \frac{1}{N}\sum_{i=1}^{N}\frac{{R_i}^4 \cdot SNR_i}{\left[\frac{3}{8} + \frac{\pi R_i}{8k\mathrm{E}(X_i)}\sin\frac{4k\mathrm{E}(X_i)}{\pi R_i} + \frac{\pi R_i}{64k\mathrm{E}(X_i)}\sin\frac{8k\mathrm{E}(X_i)}{\pi R_i}\right]G_{\max}^2 C} \tag{33}$$

In order to quantitatively evaluate the accuracy, the RCS expected measurement error $\eta_{\overline{\delta}}$ is defined as the absolute value of the ratio between the real RCS expected value $\overline{\delta_r}$ and the measured RCS expected value $\overline{\delta_m}$:

$$\eta_{\overline{\delta}} = \left|\frac{\overline{\delta_r}}{\overline{\delta_m}}\right| \tag{34}$$

The mass expectation of the insects $E(m_i)$ can be obtained by factoring the result of $\overline{\delta}$ into Equation (12). Combining Equations (3), (5), and (12), the calculation equation of the migratory insect biomass M can be obtained. The statistical precision percentage ε_M of the migratory biomass is defined as the accuracy level of the evaluation statistical method. As shown in Equation (35), ε_M is defined as the ratio of the absolute value of the difference from M_r and M_m to M_r. The closer ε_M is to 100%, the higher the accuracy of migratory biomass M will be.

$$\varepsilon_M = \frac{|M_r - M_m|}{M_r} \times 100\% \tag{35}$$

3. Results

The insect migratory biomass estimation method is introduced above. The correctness and feasibility of the proposed methods are verified by the simulation and field experiments presented in this section.

3.1. Simulation Analysis

In this section, the migratory biomass calculation model proposed in Section 2 is simulated and verified. The random crossing beam model of the insect swarm is established. The RCS expectation of the individual insect is estimated through simulation, and the migratory biomass is estimated through simulation.

3.1.1. RCS Expectation Accuracy Simulation

Suppose that the radar works in the vertical-looking mode, and *Num* migrating insects randomly cross the beam. The migratory flux is calculated according to the model designed in Section 2. The results are compared with the theoretical values to verify the correctness and confidence interval of the method.

The RCS v_i of *Num* migrating insects are assumed to obey a normal distribution, with the mean value E $= -45$ dBsm and standard deviation σ $= 3$ dBsm, as shown in Figure 7a. The migrating height H_i obeys a normal distribution, with the mean value E $= 500$ m and standard deviation σ $= 50$ m, as shown in Figure 7b. The time t_i of entry into the radar beam occurs randomly within 12 h. The migrating flight speed V_i follows a normal distribution, with mean value E of 15 m/s and standard deviation σ of 3 m/s, as shown in Figure 7c. The distance Y_i from the insect I to the center of the radar beam, being normal, is assumed to obey a random uniform distribution U$[0, D_i/2]$. According to the above assumptions, the deviation coefficient μ_i and the actual crossing distance X_i can be solved. For the insect with the number i, its SNR_i can be calculated by the transformation of Equation (14), and then its $\theta_{i-\max}$ can be calculate by Equation (31). Finally, this insect's X_i is obtained. The distribution of X_i is shown in Figure 7d.

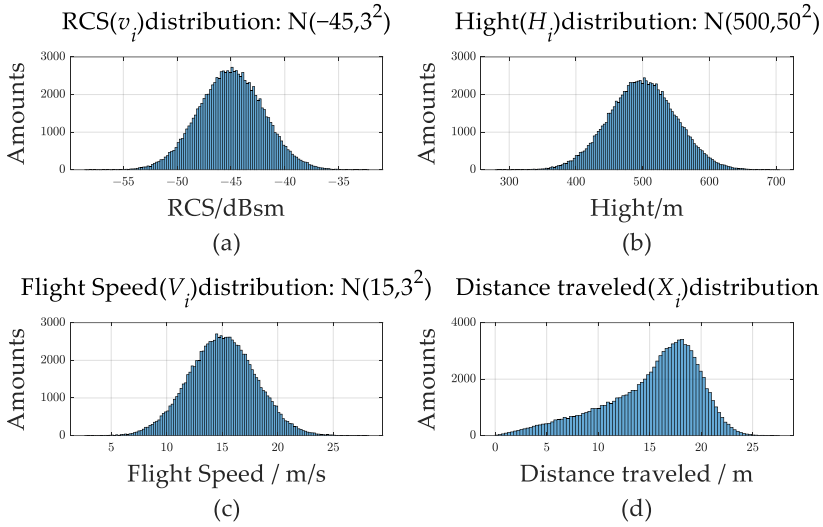


Figure 7. Simulation input conditions. (**a**) RCS v_i distribution. (**b**) Height H_i distribution. (**c**) Speed V_i distribution. (**d**) Real crossing distance X_i distribution.

Under the above conditions, the expectation and standard deviation of $\eta_{\bar{\delta}}$ in the full polarimetric entomological radar were simulated. The expectations of $\eta_{\bar{\delta}}$ of the traditional method and the new method are recorded as $E'(\eta_{\bar{\delta}})$ and $E''(\eta_{\bar{\delta}})$, respectively. Similarly, the standard deviations of $\eta_{\bar{\delta}}$ are recorded as $\sigma'(\eta_{\bar{\delta}})$ and $\sigma''(\eta_{\bar{\delta}})$, respectively. During the simulation, the difference between the two methods is that in the traditional calculation process, when calculating the RCS of a single insect, $\gamma_{i-\max}$ is set to 0 in Equation (17).

The number of statistical samples *Num* is changed from 5 to 10^5, and a 10^4 Monte Carlo simulation is conducted under each condition.

The simulation results are shown in Figure 8. Figure 8a is the expected simulation results of $\eta_{\bar{\delta}}$. Figure 8b is the standard deviation simulation results of $\eta_{\bar{\delta}}$. In Figure 8a, the blue line shows the relationship between $E'(\eta_{\bar{\delta}})$ and the number of samples *Num*, and the red line shows the relationship between $E''(\eta_{\bar{\delta}})$ and *Num*. In Figure 8b, the blue line shows the relationship between $\sigma'(\eta_{\bar{\delta}})$ and *Num*, and the red line shows the relationship between $\sigma''(\eta_{\bar{\delta}})$ and *Num*. From the results, it can be seen that the $E'(\eta_{\bar{\delta}})$ is close to 4.13 dB, which decreases gradually with the increase in *Num*. However, it does not tend towards 0 dB. $E''(\eta_{\bar{\delta}})$ converges to obtain 0.04 dB and gradually decreases with the increase in *Num*. When *Num* reaches 150, $E''(\eta_{\bar{\delta}})$ reaches 0.05 dB. This can meet the accuracy requirements for the biomass measurement. Furthermore, with the increase in *Num*, $\sigma'(\eta_{\bar{\delta}})$ and $\sigma''(\eta_{\bar{\delta}})$ all tend towards 0 dB. Through comparison, by using the new method, the measurement error $\eta_{\bar{\delta}}$ of the insect RCS expectation is significantly lower than that of the traditional method. This means the new method has a higher accuracy. The reason for the difference between the expected error values $E'(\eta_{\bar{\delta}})$ and $E''(\eta_{\bar{\delta}})$, which is about 4 dB, is that in the traditional RCS mean calculation method of the fully polarimetric entomological radar, if the factor of the insect crossing beam position is not considered, the RCS statistical results will have a large deviation. The new method proposed in this paper can effectively solve this problem.

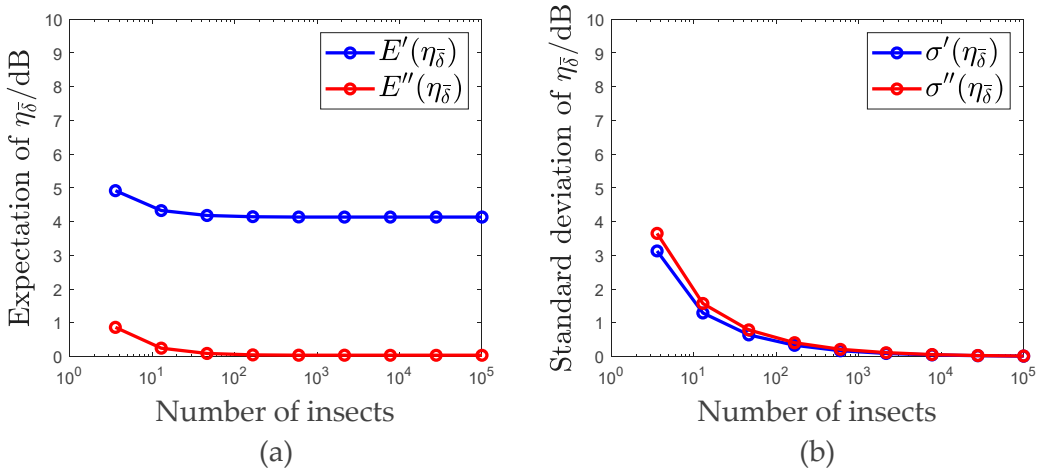


Figure 8. Comparison of the simulation results of $\eta_{\bar{\delta}}$: (**a**) expectation of $\eta_{\bar{\delta}}$; (**b**) standard deviation of $\eta_{\bar{\delta}}$.

3.1.2. Simulation of the Accuracy of the Migratory Biomass Estimation

In order to further verify the accuracy of the proposed method for estimating the migratory biomass, the results of the biomass estimation of the migrating insects are validated through simulations below. It is assumed that 10^5 insects pass through the radar beam in random spatial positions in turn. The simulation conditions are the same as those described in Section 3.1.1. The simulation conditions are shown in Figure 7. It is assumed that the radiation power of the entomological radar is sufficient, meaning that most of the insects can be detected by the radar, except for a few insects that cross the edge of the beam. The actual biomass of 10^5 insects M_r is calculated by Equation (1). Then, according to Equation (2), the migratory biomass M_m under the conditions of the traditional method and the new method are calculated, respectively.

The errors in the biomass calculation using traditional method and new method were simulated, respectively. In the traditional calculation method, the $E(m_i)$ of *Num* insects was estimated using Equations (12) and (18), with the $\gamma_{i-\max} = 0$. In the new calculation method, $E(m_i)$ was estimated using Equations (12) and (33). Then, according to Equation (2), $E(m_i)$ was multiplied by the number of detected insects *Num* to obtain the measured value of the migratory biomass M_m. With the increase in the statistical sample size *Num* from 5 to 10^5, 10^5 Monte Carlo simulations were performed under each set of *Num*

conditions. Based on Equation (35), ε_M was obtained. We can then take the expectation and standard deviation of ε_M to evaluate the statistical accuracy. The expectations of ε_M in the traditional method and the new method are recorded as $E'(\varepsilon_M)$ and $E''(\varepsilon_M)$, respectively. The standard deviations of ε_M are recorded as $\sigma'(\varepsilon_M)$ and $\sigma''(\varepsilon_M)$, respectively.

The simulation results are shown in Figure 9. Figure 9a is the expected simulation results of ε_M. Figure 9b is the standard deviation simulation results of ε_M. In Figure 9a, the blue line and red line represent the tendency of $E'(\varepsilon_M)$ and $E''(\varepsilon_M)$ with respect to *Num*, respectively. In Figure 9b, the blue line and red line represent the tendency of $\sigma'(\varepsilon_M)$ and $\sigma''(\varepsilon_M)$ with respect to *Num*, respectively. From the simulation results, it can be seen that with the increase in *Num*, $E'(\varepsilon_M)$ converges to 60% and $E''(\varepsilon_M)$ converges to 100%. $\sigma'(\varepsilon_M)$ converges to 1.2% and $\sigma''(\varepsilon_M)$ converges to 0. Using the new method, when *Num* increases to 2000, $E''(\varepsilon_M)$ reaches 98.7%, and $\sigma''(\varepsilon_M)$ is less than 0.86%, which effectively represent the scale of the migratory biomass. It can be concluded that, if $\gamma_{i-\max}$ is not taken into account, the statistical result error in the migration biomass is too large to accurately assess the migration scale.

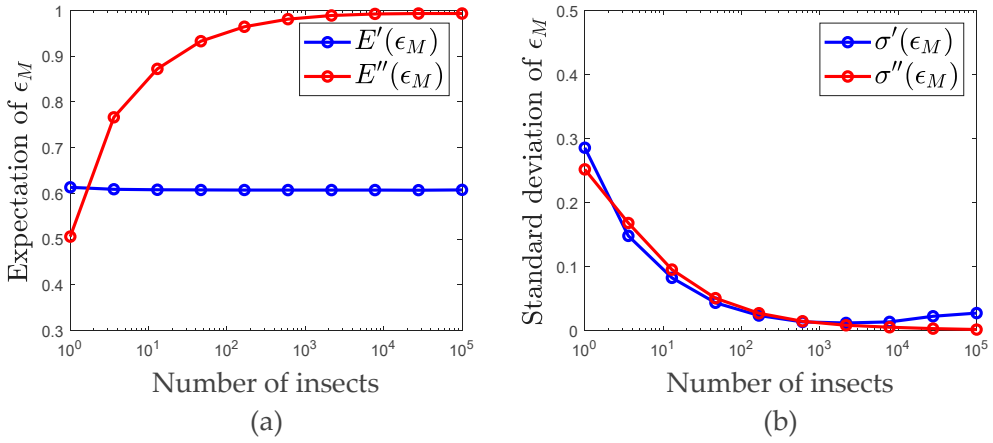


Figure 9. Comparison of the simulation results of ε_M: (**a**) expectation of ε_M; (**b**) standard deviation of ε_M.

From the simulation results shown in Figure 9a, it can be found that there is a simple proportional relationship between the true value and the error value. For the convenience of the calculation, the error value can also be directly divided by 0.6 to obtain a result close to the true value. The work described in this paper aims to establish a more reasonable, fully polarimetric entomological measurement model, and through calculation and derivation, the correct results can also be obtained.

In this section, the new method of migratory biomass measurement based on full polarimetric entomological radar is compared with the traditional method. It is verified that the method proposed in this paper has a better accuracy in estimating the RCS and biomass. At the same time, the accuracy of the migratory biomass measurement increases with the increase in the statistical sample size. The superiority of the new method for estimating the migratory biomass is verified.

3.2. Experimental Verification

In order to further verify the method of estimating the migratory biomass proposed in this paper, a full polarimetric entomological radar was used for the verification experiments. This comprises a Ku-band, high-resolution, vertical scanning dual-mode radar. The radar system applies the step frequency synthesis method to form a bandwidth of 800 MHz, which enables it to achieve a range resolution of about 0.2 m [35]. Therefore, it is easy to distinguish individual migrating insects above the radar. The radar is shown in Figure 10a. It is located in Dongying, Shandong, China, as shown in Figure 10b. It is used to monitor the activities of seasonal migrating insects. The radar was established in April 2021 and performs long-term monitoring tasks.



(**a**) (**b**)

Figure 10. Ku-band, high-resolution, fully polarimetric entomological radar. (**a**) Radar scene picture. (**b**) Satellite map of the radar installation location.

On October 8 2021, a large number of *Sarcopolia illoba* (Butler, 1878) migrated and were monitored by entomological radar. The common name of the species is mulberry caterpillar. The migratory biomass statistical method designed in this paper was used. According to Equations (12) and (33), the mass expectation of a single insect in this migration is 90.7 mg. Along with the radar, a searchlight trap was installed. This is a kind of equipment that uses the phototaxis of migrating insects to trap them. The statistic results can be used to verify the rationality of the radar measurement results, as shown in Figure 11. Figure 11a shows the installation position of the searchlight trap. It is mounted on a third-floor exterior open terrace. The terrace is about 8 m above the ground. Figure 11b shows its working scene. The searchlight trap is turned on from 18:00 p.m. to 6:00 p.m. the next day. It has a metal halide lamp with 1 kW power and was produced by Shanghai Yaming Lighting Co., Ltd.



(**a**) (**b**)

Figure 11. Searchlight trap. (**a**) Installation position. (**b**) Working scene.

On the same day, many insects were also trapped by the searchlight trap. Table 1 shows the ratios and average mass of the target species among the trapped insects. Among these insects, the ratio of *S. illoba* was the highest, reaching 87.6%. Therefore, it was a migration event dominated by *S. illoba*. Fifty *S. illoba* were randomly selected, and their masses were measured. The measured mass results range from 43.1 mg to 133.9 mg, with an average of 99 mg, as shown in Figure 12. Figure 12a shows the mass measurement results of fifty randomly selected insects, and Figure 12b shows the mass statistical distribution of these insects.

Table 1. Ratios and average mass of the target species among the trapped insects.

Insect Species	Average Mass	Quantity Proportion
Sarcopolia illoba (Butler, 1878)	99 mg	87.6%
Coccinella septempunctata (Linnaeus, 1758)	29.7 mg	7%
Apolygus lucorum (Meyer-Dür, 1843)	5.2 mg	3.2%
Gyllotalpa unispina (Sausure, 1874)	1.01 g	2.1%

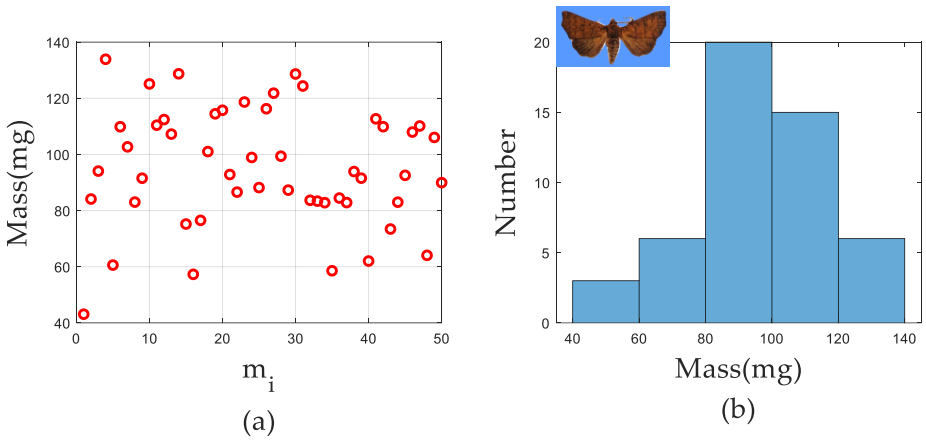


Figure 12. Statistical results of the mass measurement of the captured insects. (**a**) Mass measurement results. (**b**) Statistical results for the mass.

The estimated mass measured by the radar is 90.7 mg, and the reference mass measured using the electronic scale is 99 mg. The result has a difference of about 10%. This is because the targets measured by the radar include a small number of *Coccinella septempunctata* (Linnaeus, 1758) and *Apolygus lucorum* (Meyer-Dür, 1843), which are relatively small in mass. *Gyllotalpa unispina* (Sausure, 1874) have no effect on the radar measurement because they are active in the near-ground areas.

Then, based on the migratory flux results obtained on October 8, 2021, the migratory biomass of *S. illoba* in a wider area was estimated. The entomological radar works in the vertical-looking mode. According to the statistical method introduced in [28], the migratory flux on that day can be calculated. The results are shown in Figures 13 and 14. Figure 13 shows the *flux* with different heights and times. Figure 14 shows the time-averaged *Flux* profile for the whole day.

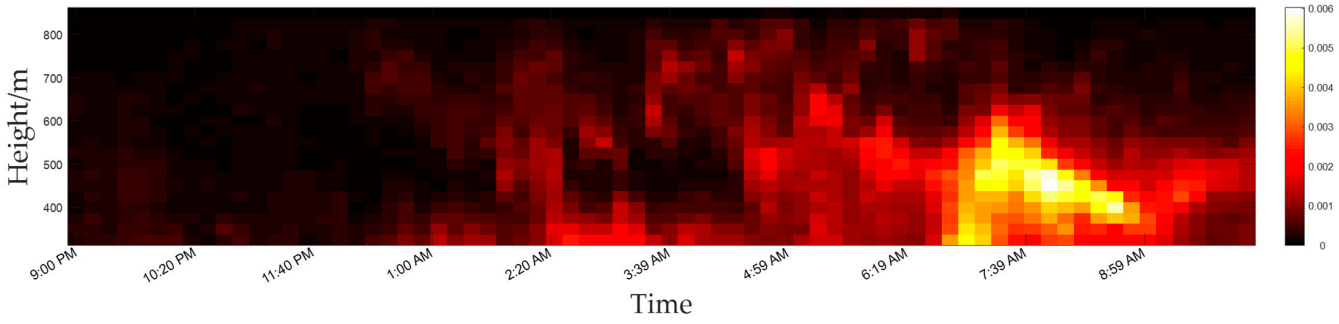


Figure 13. Migration *flux* with the height interval $\Delta h = 25$ m and time interval $\Delta T = 600$ s.

According to the migratory *flux* statistical results in Figure 13, the horizontal axis represents the time, and the vertical axis represents the height above the radar. It can be seen that between 2:00 and 5:00, the insects are concentrated over 500 m. It is estimated that the migration event is in the horizontal transportation phase during this period. During 6:00–9:00, the height of the insects decreased gradually, with an obvious landing trend. According

to the *Flux* statistical results in Figure 14, within the detection altitude range H = 500 m, from of 350 m to 850 m, the average flux of this relocation is $Flux$ = 0.000745 insects/m^2/s, and the duration is 12 h from 9:00 p.m. to 9:00 a.m. According to Equations (12) and (33), it can be calculated that about 1.4598 tons of *S. illoba* migrated within a regional range of L = 1 km and an altitude range of H = 500 m.

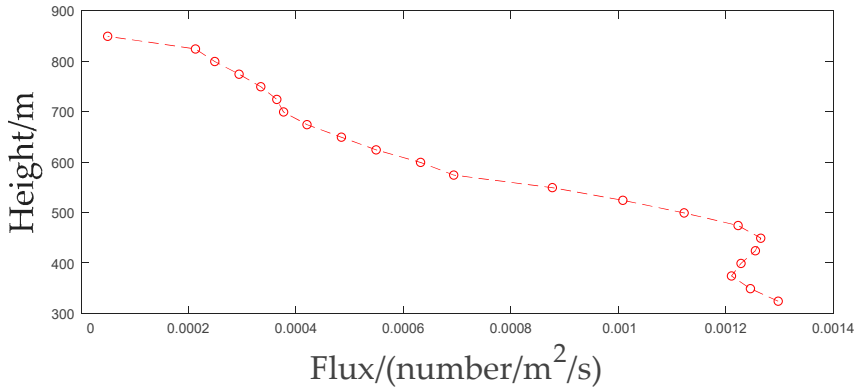


Figure 14. Height–average *Flux* profile measured.

As shown in Figure 2, L represents the width of the plane over which insects migrate, and it describes the diffuse region of the insects during the migration. Since there are no more searchlight traps or entomological radars installed in this area, the estimated value of the migratory biomass within 1 km is given here. The regional range of 1 km does not represent the total migration scale of the *S. illoba*. In order to obtain a more accurate L, further research should be carried out to expand the monitoring scope in the future. More searchlight traps or entomological radars should be installed in a larger area to judge the migration scale in large areas.

4. Discussion

The basic principle of measuring the insect mass using fully polarimetric entomological radar is to measure the RCS of the insect and then estimate its mass based on the mapping relationship between the mass and RCS [11,12]. For the fully polarimetric entomological radar without the capacity for in-beam angle measurement, all the insects are measured based on the assumption that they all pass through the center of the radar beam. This leads to large RCS measurement errors, because most of the detected insects do not cross the beam center. Therefore, the estimated insect mass and migratory biomass are usually calculated with large errors based on the traditional method. A new method was designed in this paper to solve this problem. The method is used to calculate a more accurate average RCS based on the assumption that at a certain height in a small area, the insects are uniformly distributed. Compared with the traditional method for fully polarimetric entomological radar, this method has a better accuracy in terms of the statistics of the migratory biomass. Using VLR-type entomological radar, it is easy to obtain the position of the insects in the beam by the rotating polarization and nutation method. Then, the mass and biomass of insects can be obtained. The advantage lies in the direct measurement, with the biomass measurement accuracy depending on the insect individual mass measurement accuracy. In this paper, the average mass of a migratory species of insects is estimated, and the biomass of a region is calculated based on the flux results. This solves the problem of measuring the biomass using entomological radar without the angle measurement in regard to the beam and provides a new concept for estimating the migratory biomass in a larger area. When estimating the biomass in a large area, if the entomological radar works in the vertical-looking mode, it is necessary to assume that the migratory flux of the insects in the area is uniform.

If a more accurate migratory biomass measurement is to be carried out in a larger area, two methods should be used. One method is to set up more entomological radars on the insect migration belt to increase the spatial sampling rate of the migrating insects. Another method is to use the scanning mode of the entomological radar to measure the flux of the insects in the cross-section of the migration direction. Combined with the individual mass estimation method designed in this paper, the total biomass of migratory insects can be estimated more accurately.

The biomass estimation method designed in this paper for fully polarimetric entomological radar has two limitations in terms of its application. Firstly, it is applicable to mono-species migration events or various insect species of a similar size. Migration event involving different sizes (mass) and numbers of various insects often occur. Therefore, it is necessary to preliminarily filter the detected insects by species using the method of species recognition. Cheng Hu et al. (2018) proposed a decision tree support vector machine method for classifying migrating insects [19]. In the future, the application of biomass estimations will be expanded through a species classification algorithm. Secondly, the insects could be in the Ku-band radar′s optical, Raleigh, or Mie-scattering regions. The insect mass inversion calculation needs to meet its size in the Rayleigh region. At present, there is no suitable computational method that can be used to solve the ambiguity in the cross-scattering region mass calculation. From the capture information based on the insect searchlight traps, one can infer whether or not the insect species size belongs to the Ku-band inversion interval. This problem could be solved in the future by replacing the X-band entomological radar, because the mass inversion interval of the insects in the X-band is larger, covering most of the migratory insect species.

5. Conclusions

The migratory biomass is of great significance for pest control and ecological environment research. In this paper, a method of measuring the insect migratory biomass by fully polarimetric entomological radar was proposed. Without measuring the position of the insects in the radar beam, the mass expectation of an individual insect can be estimated using the statistical method. Combined with the statistical results for the migratory flux, the insect migratory biomass within a regional range can be estimated. The simulation results verify the effectiveness of the method. Compared with the traditional method, the new method greatly improves the accuracy of the insect mass expectation estimation without the need for angle measurement information on the insects. The influence of the statistical samples on the accuracy of the method was also analyzed through simulations, and it is concluded that the increase in the number of statistical samples can improve the estimation accuracy of the method. In addition, Ku-band, high-resolution, fully polarimetric entomological radar and searchlight traps set up in the field were used to verify the effectiveness of this method.

Author Contributions: T.Y. developed the method and wrote the manuscript; T.Y., T.Z., and W.L. designed and carried out the experiments; and M.L., W.L., R.W. and C.H. reviewed and edited the manuscript. All authors have read and agreed to the published version of the manuscript.

Funding: This research was funded by the Special Fund for Research on National Major Research Instruments under grant No. 31727901; the Major Scientific and Technological Innovation Project (2020CXGC010802); and the National Natural Science Foundation of China (grant No. 62001021).

Institutional Review Board Statement: Not applicable.

Informed Consent Statement: Not applicable.

Data Availability Statement: Not applicable.

Conflicts of Interest: The authors declare no conflict of interest.

References

1. Holland, R.A.; Wikelski, M.; Wilcove, D.S. How and why do insects migrate? *Science Mad.* **2006**, *313*, 794–796. [CrossRef] [PubMed]
2. Hahn, S.; Bauer, S.; Liechti, F. The natural link between Europe and Africa–2.1 billion birds on migration. *Oikos* **2009**, *118*, 624–626. [CrossRef]
3. Chapman, J.W.; Nesbit, R.L.; Burgin, L.E.; Reynolds, D.R.; Smith, A.D.; Middleton, D.R.; Hill, J.K. Flight orientation behaviors promote optimal migration trajectories in high-flying insects. *Science* **2010**, *327*, 682–685. [CrossRef] [PubMed]
4. Chapman, J.W.; Bell, J.R.; Burgin, L.E.; Reynolds, D.R.; Pettersson, L.B.; Hill, J.K.; Bonsall, M.B.; Thomas, J.A. Seasonal migration to high latitudes results in major reproductive benefits in an insect. *Proc. Natl. Acad. Sci. USA* **2012**, *109*, 14924–14929. [CrossRef] [PubMed]
5. Chapman, J.W.; Reynolds, D.R.; Wilson, K. Long-range seasonal migration in insects: Mechanisms, evolutionary drivers and ecological consequences. *Ecol. Lett.* **2015**, *18*, 287–302. [CrossRef]
6. Kays, R.; Crofoot, M.C.; Jetz, W.; Wikelski, M. Terrestrial animal tracking as an eye on life and planet. *Science* **2015**, *348*, aaa2478. [CrossRef]
7. Warrant, E.; Frost, B.; Green, K.; Mouritsen, H.; Dreyer, D.; Adden, A.; Brauburger, K.; Heinze, S. The Australian Bogong moth Agrotis infusa: A long-distance nocturnal navigator. *Front. Behav. Neurosci.* **2016**, *10*, 77. [CrossRef]
8. Hu, G.; Lim, K.S.; Horvitz, N.; Clark, S.J.; Reynolds, D.R.; Sapir, N.; Chapman, J.W. Mass seasonal bioflows of high-flying insect migrants. *Science* **2016**, *354*, 1584–1587. [CrossRef]
9. Wilcove, D.S.; Wikelski, M. Going, going, gone: Is animal migration disappearing. *PLoS Biol.* **2008**, *6*, e188. [CrossRef]
10. Bauer, S.; Hoye, B.J. Migratory animals couple biodiversity and ecosystem functioning worldwide. *Science* **2014**, *344*, 1242552. [CrossRef]
11. Landry, J.S.; Parrott, L. Could the lateral transfer of nutrients by outbreaking insects lead to consequential landscape-scale effects? *Ecosphere* **2016**, *7*, e01265. [CrossRef]
12. Zhang, Z.; Zhang, Y.; Jiang, Y.; Wang, J.; Xie, A.; Yang, J. Current status of entomological radar development and application prospect in China. *China Plant Prot. J.* **2017**, *37*, 27–32.
13. Hu, G.; Gao, B.; Feng, H.; Jiang, H.; Zhai, P.; Wu, K. Individual behavior, population dynamics and ecological effects of migrating insects. *J. Chin. Sci. Found.* **2020**, *34*, 456–463.
14. Oerke, E.C. Crop losses to pests. *J. Agr. Sci. Camb.* **2006**, *144*, 31–43. [CrossRef]
15. Bebber, D.P.; Holmes, T.; Gurr, S.J. The global spread of crop pests and pathogens. *Global Ecol. Biogeogr.* **2014**, *23*, 1398–1407. [CrossRef]
16. Zhai, B. Tracking angels—30 years of radar entomology. *Acta Entomol. Sin.* **1999**, *42*, 315–326.
17. Drake, V.A. *Quantitative Observation and Analysis Procedures for a Manually Operated Entomological Radar*; CSIRO: Melbourne, Australia, 1981.
18. Wang, R.; Li, W.D.; Hu, C.; Li, M.Y.; Mao, H.F. Full-polarization entomological radar bioparametric inversion method and quantitative experimental validation in the external field. *J. Signal. Process.* **2021**, *37*, 199–208. [CrossRef]
19. Hu, C.; Kong, S.; Wang, R.; Long, T.; Fu, X. Identification of Migratory Insects from their Physical Features using a Decision-Tree Support Vector Machine and its Application to Radar Entomology. *Sci. Rep.* **2018**, *8*, 5449. [CrossRef]
20. Chapman, J.; Smith, A.; Woiwod, I.; Reynolds, D.; Riley, J. Development of vertical-looking radar technology for monitoring insect migration. *Comput. Electron. Agric.* **2002**, *35*, 95–110. [CrossRef]
21. Chapman, J.W.; Reynolds, D.R.; Smith, A.D. Vertical-Looking Radar: A New Tool for Monitoring High-Altitude Insect Migration. *BioScience* **2003**, *53*, 503–511. [CrossRef]
22. Wang, R.; Hu, C.; Liu, C.; Long, T.; Kong, S.; Lang, T.; Gould, P.J.L.; Lim, J.; Wu, K. Migratory Insect Multifrequency Radar Cross Sections for Morphological Parameter Estimation. *IEEE Trans. Geosci. Electron.* **2019**, *57*, 3450–3461. [CrossRef]
23. Hu, C.; Kong, S.; Wang, R.; Zhang, F. Radar Measurements of Morphological Parameters and Species Identification Analysis of Migratory Insects. *Remote Sens.* **2019**, *11*, 1977. [CrossRef]
24. Hu, C.; Kong, S.; Wang, R.; Zhang, F.; Wang, L. Insect Mass Estimation Based on Radar Cross Section Parameters and Support Vector Regression Algorithm. *Remote Sens.* **2020**, *12*, 1903. [CrossRef]
25. Cai, J.; Yuan, Q.; Wang, R.; Liu, C.; Zhang, T. Insect detection and density estimation based on a Ku-band scanning entomological radar. *J. Eng.* **2019**, *2019*, 7636–7639. [CrossRef]
26. Chao, Z.; Rui, W.; Hu, C. Equivalent Point Estimation for Small Target Groups Tracking based on MLE. *Sci. China Inf. Sci* **2019**, *63*, 8.
27. Hu, C.; Li, W.; Wang, R.; Li, Y.; Li, W.; Zhang, T. Insect flight speed estimation analysis based on a full-polarization radar. *Sci. China Inf. Sci* **2018**, *61*, 1–3. [CrossRef]
28. Yu, T.; Li, M.; Li, W.; Cai, J.; Wang, R.; Hu, C. Insect Migration Flux Estimation Based on Statistical Hypothesis for Entomological Radar. *Remote Sens.* **2022**, *14*, 2298. [CrossRef]
29. Aldhous, A.C. An investigation of the polarisation dependence of insect radar cross sections at constant aspect. Cranfield University: Cranfield, UK, 1989.
30. Li, W.D.; Wang, R.; Hu, C.; Zhang, N.; Liang, W.Z. Ku-band fully polarimetric radar insect body shape parameter inversion. *Acta Elect Ronica Sin.* **2021**, *49*, 1241–1248.

31. Hu, C.; Li, W.; Wang, R.; Long, T.; Liu, C.; Drake, V.A. Insect Biological Parameter Estimation Based on the Invariant Target Parameters of the Scattering Matrix. *IEEE Trans. Geosci. Electron.* **2019**, *57*, 6212–6225. [CrossRef]
32. Li, W.; Hu, C.; Wang, R.; Kong, S.; Zhang, F. Comprehensive analysis of polarimetric radar cross-section parameters for insect body width and length estimation. *Sci. China Inf. Sci.* **2021**, *64*, 11. [CrossRef]
33. Hu, C.; Li, M.; Li, W.; Wang, R.; Yu, T. A Data-Driven Polarimetric Calibration Method for Entomological Radar. *IEEE Trans. Geosci. Electron.* **2022**, *60*, 1–14. [CrossRef]
34. Song, X.J. Polarization feature-based radar target recognition technique. *Radar Sci. Technol.* **2016**, *14*, 7.
35. Yu, T.; Li, M.; Li, W.; Mao, H.; Wang, R.; Hu, C.; Long, T. Polarimetric Calibration Technique for a Fully Polarimetric Entomological Radar Based on Antenna Rotation. *Remote Sens.* **2022**, *14*, 1551. [CrossRef]